MASW Survey Using Multiple Source Offsets

Choon B. Park, Park Seismic, LLC, Shelton, Connecticut, USA
JB Shawver, Zonge Geosciences, Inc., Minneapolis, Minnesota, USA

Abstract

Although it is generally known that the active MASW method tends to average out the near-field effect of surface waves through the slant-stack process implicitly incorporated in dispersion imaging and therefore one optimum source offset (X1) is usually employed for a given survey, a long source offset to ensure recording of long wavelengths can sometimes result in a lack of short-wavelength energy due to excessive attenuation and, on the other hand, the use of a short source offset can result in the opposite consequence. To reduce this ambiguity, we propose acquisition of field data with multiple source offsets; for example, X11=1dx, X12=(N/4)dx, X13=(N/2)dx, etc., at a given location of N-channel receiver spread with dx separation. Then, each set of field data is separately processed for dispersion image, resulting in multiple set of dispersion image data for a given measurement location. These image data sets are then stacked on top of each other to produce a single image data set for a location, where the fundamental mode (M0) dispersion curve is usually identified through a broader bandwidth with lower frequencies and improved accuracy via multi-modal delineation of dispersion trends. This approach can make the final 2-D shear-velocity (Vs) map image deeper with a broader depth range and improved accuracy.

Introduction

Clarification of the optimum offset concept for the active MASW method requires a comprehensive understanding about the surface wave propagation and the lateral resolution limit of the method, both of which are continuously evolving and updated by practitioners and researchers. The near-field effect of surface wave propagation tells us the measurement should take place a certain distance away from the source point due to the excessive stress-strain environment that prohibits the generation of stable planar surface waves (Richart et al., 1970; Stokoe et al., 1994; Gucunski and Woods, 1991; Park et al., 1999). Although the exact distance (d_c) to avoid this adverse effect is still a debatable issue, the unanimous observation indicates that it changes with wavelength (λ): a longer λ requires a longer d_c (Figure 1). On the other hand, although a clear theory and a unanimous standard are also not available yet for lateral resolution limit with MASW, the most

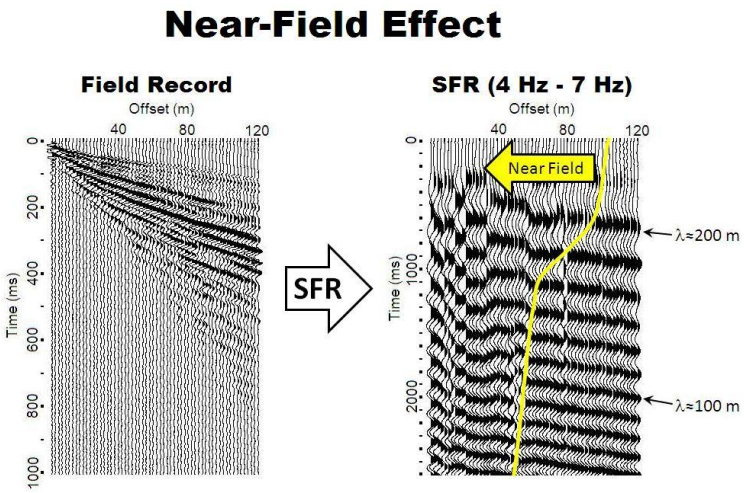

Figure 1. A field record (left) and its swept-frequency record (SFR) (Park et al., 1999) for a frequency of 3 Hz - 6Hz range, showing the minimum distance (dc) to avoid the near-field effect changes with wavelength.

fundamental principle tells us that, for a fixed number of receivers (N), a longer receiver spread (L) will decrease the lateral resolution. Then, a shorter spread to maintain the lateral resolution directly conflicts with the opposite requirement of a longer spread to achieve (1) deeper investigation depth (Zmax) (Stokoe et al., 1994; Park et al., 1999), and (2) higher accuracy in dispersion imaging (Park et al., 2001).

To address the near-field effect most accurately, the active MASW survey has to use varying source offsets (X1's) for different frequencies (wavelengths) measured. Because this is not a viable option in reality and also because the slant-stack processing implicitly incorporated in the dispersion imaging scheme tends to cancel out those irregular and nonlinear arrival patterns caused by the near-field effect (Figure 1), one optimal X1 is usually adopted for a given survey as a trade-off. Or, an excessively long receiver spread along with an acquisition system with an excessive number of channels (e.g., ≥ 48 channels) is sometimes adopted to ensure the widest range of X1's covered by the survey, sacrificing the significant lateral resolution. On the other hand, although an optimal X1 based on a certain empirical criterion (e.g., X1 ≥ 0.5L, X1 ≥ 0.5Zmax, etc.) has been used as the most common and practical solution (Stokoe et al., 1994; Gucunski and Woods, 1991; Park et al., 1999), there is no guarantee that it is free of adverse influence from the near-field effect. Park and Ryden (2007) proposed a data-processing effort to reduce both near- and far-field effects during the dispersion imaging. Effectiveness of any post-acquisition effort, however, will be limited by the status of the acquired data, and therefore the field approach, if possible, should be considered with highest priority.

We propose a relatively simple field effort that can further reduce the effect of the near-field effect that, for a given receiver spread, delivers multiple impacts at several different source offsets (X1's) before the spread moves to the next measurement location. With this approach, each set of data with the same source offset is then processed separately for dispersion imaging. Multiple sets of dispersion image data are then stacked according to the surface location of the field records used for the imaging. The premise for this stacking is that these dispersion images are subject to the same dispersion phenomenon (of fundamental and higher modes) because of the common subsurface materials their constituent surface waves had propagated through, but each individual set of images has different frequency ranges and modes of prominence due to the different source distances used.

Field Survey with Multiple Source Offsets (X1's)

An active MASW survey was planned for a site characterization for the maximum depth (Zmax) of 50 ft or more. Because investigation of the shallow depth (e.g., ≥ 5 ft) was also important, there was an ambiguity in the selection of the optimum offsets during the survey planning stage. While a 5-ft

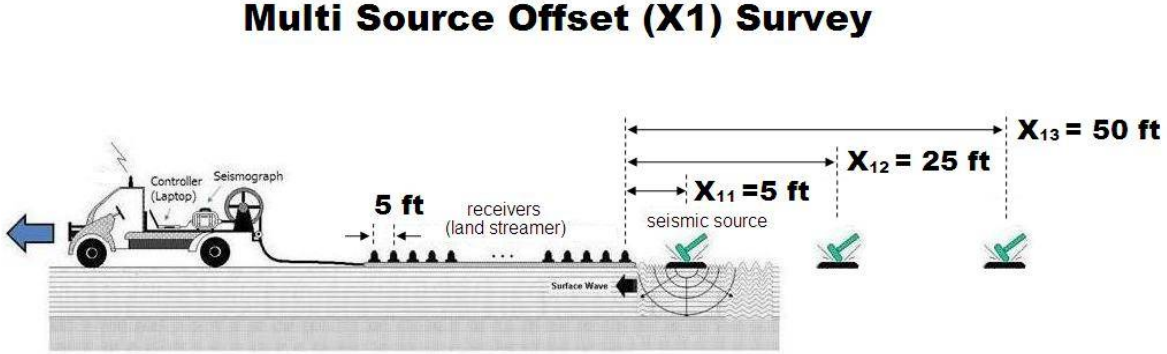

Figure 2. A schematic showing the layout of a field survey with multiple source offsets at one location on a 5-ft spacing receiver spread that continuously moved by 5 ft after finishing data collection at one location.

receiver spacing with a 24-channel acquisition system seemed optimal to ensure the Zmax (≥ 50 ft), determination of the optimal source offset (X1) faced an uncertainty that a short X1 (e.g., 5 ft) to ensure the shallow investigation would put the deeper investigation at risk, or vice versa. Instead of running multiple surveys with different X1's, multiple impacts were made at three different source offsets (X11=5 ft, X12=25 ft, and X13=50 ft) at a given location with receiver spread before the spread moved to the next measurement location, saving three different field records separately (Figure 2). In this way, three sets of data were prepared. In addition, another set of records (to be called walkaway data hereafter) was created by adding further-offset traces from records X12 and X13 after the furthest trace of X11, similar to how a walkaway record is compiled.

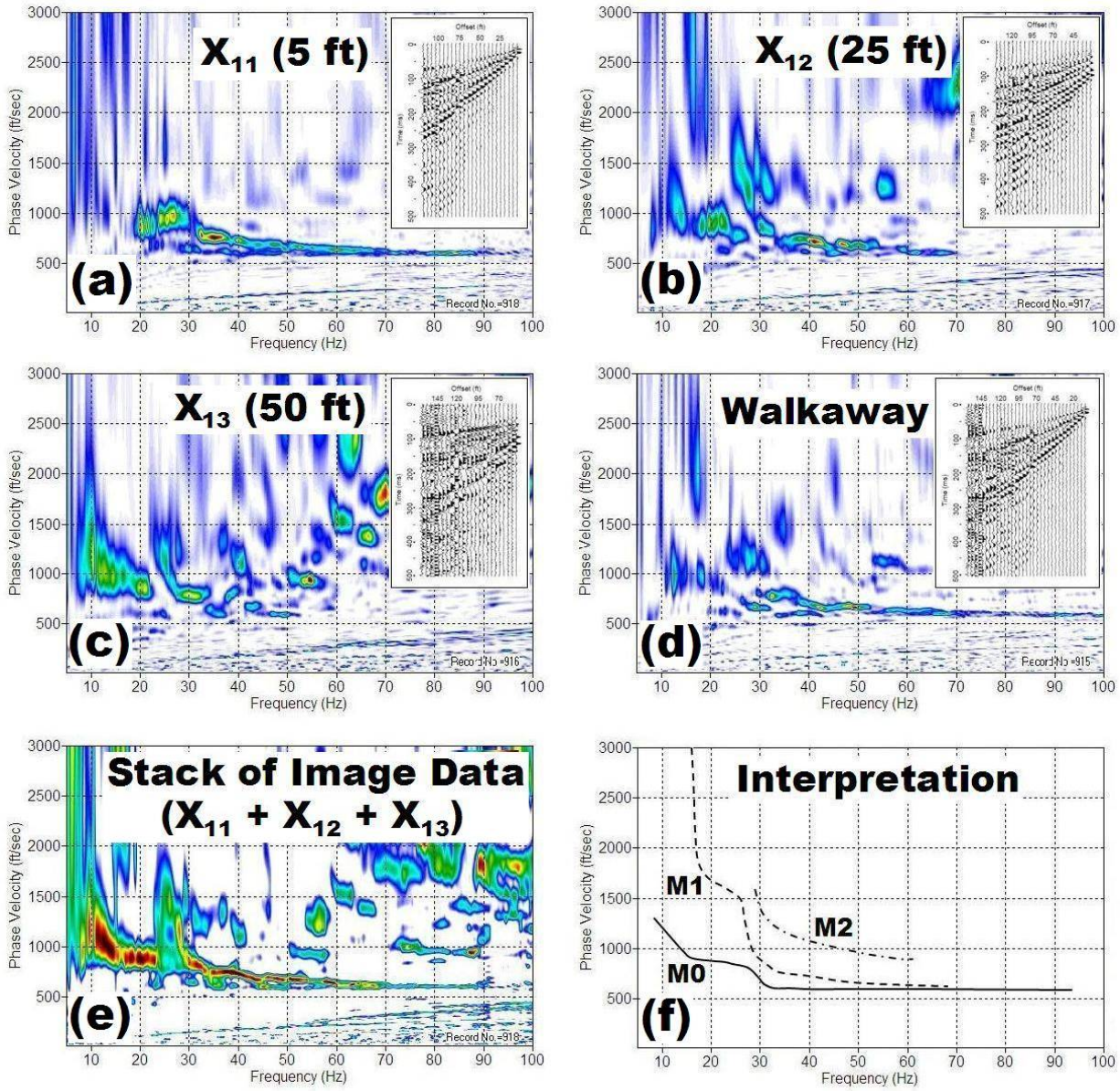

Figure 3. An example of dispersion image from each set of data with source offsets of (a) X11=5 ft, (b) X12=25 ft, and (c) X13=50 ft, respectively. Image of the walkaway record compiled from three records used for images in (a)-(c) is shown in (d). Stack of image data in (a)-(c) is shown in (e) and its interpretation is shown in (f). Constituent field records used to construct the image are shown as insets.

Data Handling

Each set of data with different X1's and the walkaway data set were then processed separately for dispersion images by using the method by Park et al. (1998), generating accordingly many sets of dispersion images. Examples from each image data set for the same receiver spread are shown in Figures 3a-3d. Another set of image data was created by stacking the image data from the three X1's of the same receiver spread locations. Figure 3e shows an example created by stacking the images shown in Figures 3a-3c.

The dispersion image from the shortest source offset (X11=5 ft) shows the prominent dispersion trends at relatively high frequencies, while the image from the longest source offset (X13=50 ft) shows those trends focused in relatively lower frequencies with the image from the intermediate source offset (X12=25 ft) falling between the two.

It is obvious multi-modal dispersion trends are associated with all these images with different excitabilities at different frequencies. The walkaway image shows these complicated trends in the highest resolution, indicating a possibility of the most effective multi-mode inversion. On the other hand, the stacked image shows those trends identifiable in the broadest bandwidth with the strongest energy imparted mostly into the fundamental mode (M0) trend.

Two sets of dispersion curves were extracted from the two image data sets with one set of curves from each set shown in Figures 3a (X11=5 ft) and 3e (the stacked image), respectively. Their subsequent inversion produced two 2-D Vs maps shown in Figures 4a and 4b, respectively. The Vs map from the stacked image data set (Figure 4b) shows a depth of analysis about twice as deep (Zmax) as that from the shortest source offset of 5 ft, due to the lower frequencies imaged. The Vs image for the common depth range (5 ft to 35 ft) appears to be slightly different from the other two. Although it is not possible at this stage of manuscript preparation to judge which is more accurate because other

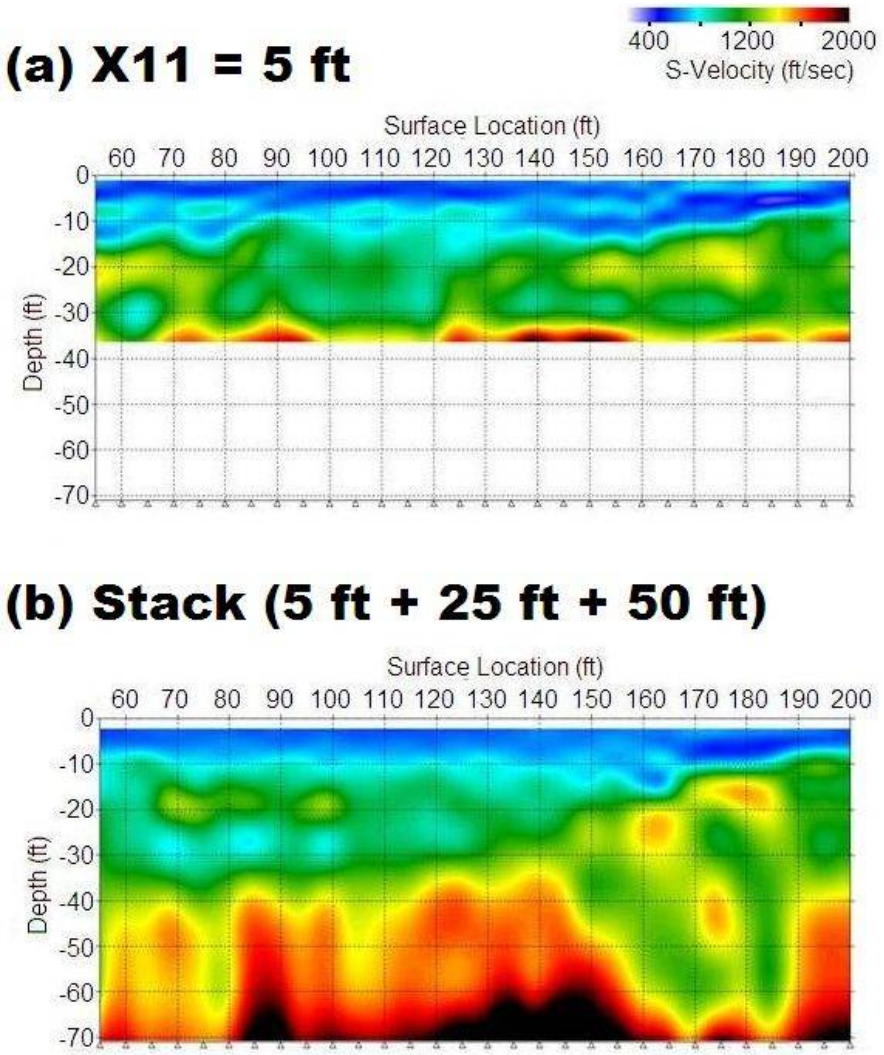

Figure 4. 2-D shear-velocity (Vs) maps constructed from two sets of dispersion curves extracted from image data sets of (a) X11=5 ft, and (b) stacking three sets of image data with X11=5 ft, X12=25 ft, and X13=50 ft.

site information is unavailable, it is believed the latter has more favorable results because of the increased accuracy during the M0-curve extraction facilitated by more comprehensive dispersion trends.

Discussion

Although it can also be an alternative approach to extract dispersion curves in different ranges from image data sets of different X1's and then merge them together to generate a curve of broader bandwidth, the approach of stacking the image data sets first and then extracting the curve form the stacked image outlined in this manuscript is much simpler, resulting in an enhanced accuracy of the extracted M0 curve, which in turn is a result of the comprehensive identification of dispersion trends on the stacked image. It was demonstrated that the longer X1 enables dispersion imaging at lower frequencies (longer wavelengths). However, the maximum wavelength imaged is about the same as the receiver spread length (aperture size of the measurement). The issues of how many different X1's are optimal and at what distances they should be are still left for further investigation theoretically and empirically. However, using multiple X1's (even only two different X1's) should benefit in any case. We recommend two or three different X1's from X11=1dx, X12=(N/4)dx, and X13=(N/2)dx be used (where N=number of channels used) for a given survey. Sometimes, stacking images from only two different X1's (for example, X11 and X13) can result in a superior image, while stacking all four sets of images (X11, X12, X13, and the walkaway) can give the best result. All these loose-ended criteria will be tightened as further studies are undertaken in the future.

Conclusions

Acquiring active MASW data with different source offsets at a given location of the receiver spread can result in a 2-D Vs map of a greater depth range and an improved accuracy both of which come from stacking dispersion image data sets processed from individual field data sets of different source offsets. This is because dispersion trends are imaged for a broader bandwidth with multi-modal details in the stacked image.

References

Gucunski, N., and Woods, R.D., 1991, Instrumentation for SASW testing, *in* S.K. Bhatia, and G.W. Blaney, eds., Recent Advances in Instrumentation, Data acquisition and testing in soil dynamics: Am. Soc. Civil Eng., 1–16.

Park, C.B., and Ryden, N., 2007, Offset selective dispersion imaging (OSDI): Proceedings of the SAGEEP 2007, Denver, Colorado, April 1-5.

Park, C.B., Miller, R.D., and Xia, J., 2001, Offset and resolution of dispersion curve in multichannel analysis of surface waves (MSW): Proceedings of the SAGEEP 2001, Denver, Colorado, SSM-4.

Park, C.B., Miller, R.D., and Xia, J., 1999, Multi-channel analysis of surface waves (MASW): Geophysics, 64, 800-808.

Park, C.B., Miller, R.D., and Xia, J., 1998, Imaging dispersion curves of surface waves on multi-channel record [Exp. Abs.]: Soc. Explor. Geophys., 1377-1380.

Richart, F.E., Hall, J.R., and Woods, R.D., 1970, Vibrations of Soils and Foundations: Prentice-Hall.

Stokoe II, K.H., Wright, S.G., Bay, J.A., and Roesset, J.M., 1994, Characterization of geotechnical sites by SASW method: *in* R.D. Woods, ed., Geophysical Characterization of Sites: Oxford Publications, New Delhi.